Acta Crystallographica Section D
Biological Crystallography
ISSN 0907-4449

Structure of the type I L-asparaginase from the hyperthermophilic archaeon *Pyrococcus horikoshii* at 2.16 Å resolution

Min Yao, Yoshiaki Yasutake, Hazuki Morita and Isao Tanaka*

Division of Biological Sciences, Graduate School of Science, Hokkaido University, Kita-10, Nishi-8, Kita-ku, Sapporo, Hokkaido 060-0810, Japan

Correspondence e-mail: tanaka@castor.sci.hokudai.ac.jp

Received 4 October 2004
Accepted 13 December 2004

PDB Reference: PhA, 1wls, r1wlssf.

The crystal structure of the L-asparaginase from the hyperthermophilic archaeon *Pyrococcus horikoshii* (PhA) was determined by the multiwavelength anomalous diffraction (MAD) method and was refined to a resolution of 2.16 Å with a crystallographic *R* factor and free *R* factor of 21.1 and 25.3%, respectively. This is the first report of the three-dimensional structure of a type I L-asparaginase. These enyzmes are known as cytosolic L-asparaginases with lower affinities for substrate than the type II L-asparaginases. Although the overall fold of PhA was closely related to the structure of the well characterized type II L-asparaginase, structural differences were also detected. PhA forms a homodimer that corresponds to half the homotetramer of type II L-asparaginases. Structure comparison at the active site reveals that most catalytic residues are conserved except for two residues that recognize the amino group of the substrate. Additionally, a remarkable structural difference is found in the so-called 'active-site flexible loop'. In PhA this loop is stabilized by β-hairpin formation and by elaborate interactions with the type-I-specific α-helical region derived from the other subunit forming the PhA dimer. The flexible loop of the type II enzyme is considered to serve as a mobile gate to the active site. Therefore, the loop stabilization observed in the PhA structure may cause limitation of the access of the substrate to the active site.

1. Introduction

L-Asparaginase (L-asparagine amidohydrolase; EC 3.5.1.1) is an enzyme that primarily catalyzes the hydrolysis of L-asparagine to L-aspartate and ammonia. *Escherichia coli* is known to contain two distinct L-asparaginase isozymes, referred to as type I and type II. *E. coli* type II L-asparaginase (EcA-II) was found to be localized in the periplasm and to have higher affinity for L-asparagine than the type I isozyme (EcA-I) (Cedar & Schwartz, 1967). The EcA-II exhibits antitumour activity (Mashburn & Wriston, 1964; Schwartz *et al.*, 1966) and has been used as a drug in the treatment of acute childhood lymphoblastic leukaemia, although the treatment is restricted owing to its multiple inflammatory or allergic side effects (Geuenich *et al.*, 1998). The mechanism of the antitumour activity of EcA-II has not yet been completely elucidated.

A number of structural studies on EcA-II (Swain *et al.*, 1993; Palm *et al.*, 1996; Jaskólski *et al.*, 2001; Sanches *et al.*, 2003) and the closely related enzymes *Erwinia chrisanthemi* L-asparaginase (ErA; Miller *et al.*, 1993; Aghaiypour *et al.*, 2001*a*,*b*; Lubkowski *et al.*, 2003), *Acinetobacter glutaminasificans* glutaminase-asparaginase (AgGA; Lubkowski, Wlodawer, Housset *et al.*, 1994), *Pseudomonas* 7A glut-

aminase-asparaginase (P7GA; Lubkowski, Wlodawer, Ammon *et al.*, 1994; Jakob *et al.*, 1997; Ortlund *et al.*, 2000) and *Wolinella succinogenes* L-asparaginase (WsA; Lubkowski *et al.*, 1996) have been carried out and a total of 24 refined crystal structures are now available in the Protein Data Bank for substrate-free forms, various complexes, mutants and reaction intermediates. All these enzymes consist of ~330 amino-acid residues and share ~40% sequence identity. The crystal structures also revealed that the enzymes form a stable homotetramer that has been described as a 'dimer of intimate dimers' (Swain *et al.*, 1993) having 222 point-group symmetry. The active-site pocket lies at the intersubunit interface of the intimate dimer and is formed from residues that are asymmetrically donated by both subunits. Therefore, the homotetramer contains four independent catalytic sites. In early crystallographic studies on EcA-II, the nine residues Thr12, Tyr25, Ser58, Gln59, Thr89, Asp90, Lys162, Asn248′ and Glu283′ were found to be included in the active site and to play a role in substrate recognition and catalysis (prime signs indicate that the residues are derived from the other subunit of the intimate dimer; Swain *et al.*, 1993). Most of these residues are conserved in the sequences of EcA-II-related type II enzymes. Numerous structural and kinetic studies have demonstrated that the catalytic reaction proceeds through the two-step ping-pong mechanism observed in serine protease (Röhm & Van Etten, 1986) and that the Thr12 residue is the first attacking nucleophile, although the activation mechanism of the weak nucleophilicity of the threonine residue is not very clear (Aghaiypour *et al.*, 2001*a*,*b*).

Table 1
Data-collection and refinement statistics.

The values in parentheses refer to data in the highest resolution shell.

	Form I (MAD)			
Form II	Peak	Edge	Remote	
Data collection				
Space group	$P2_12_12$			$P2_12_12$
Unit-cell parameters (Å)	a = 126.0, b = 76.5, c = 102.2			a = 125.7, b = 77.2, c = 98.7
Beamline	BL38B1, SPring-8			BL41XU, SPring-8
Resolution (Å)	50–2.64 (2.73–2.64)	50–2.62 (2.71–2.62)	50–2.70 (2.80–2.70)	50–2.16 (2.24–2.16)
Wavelength (Å)	0.9792	0.9794	0.9000	0.9800
R_{sym}† (%)	13.4 (39.5)	12.2 (40.2)	12.6 (39.6)	11.2 (36.0)
Completeness (%)	100.0 (100.0)	100.0 (100.0)	100.0 (100.0)	100.0 (99.9)
Unique reflections	30116	30850	28266	52174
$I/\sigma(I)$	6.2 (2.4)	6.1 (2.3)	5.9 (2.4)	7.7 (2.4)
Multiplicity	6.2 (6.4)	6.1 (6.3)	6.1 (6.3)	4.9 (4.8)
Phasing statistics				
Resolution range (Å)			25–2.62	
FOM (centric/acentric)‡			0.42/0.52	
FOM after phase improvement‡			0.95	
Refinement statistics				
Resolution range (Å)				39.48–2.16
No. of reflections				51970
R_{work}§ (%)				21.1
R_{free}¶ (%)				25.3
Total protein atoms				5094
Total water atoms				250
Average B factor (Å^2)				29.8
Model quality: r.m.s. deviation from ideality				
Bond lengths (Å)				0.018
Bond angles (°)				1.93
Dihedral angles (°)				24.88
Improper angles (°)				1.19
Ramachandran plot: residues in				
Most favoured regions (%)				85.6
Additional allowed regions (%)				13.7
Generously allowed regions (%)				0.7

† $R_{sym} = \sum_h \sum_i |I_{h,i} - \langle I_h \rangle| / \sum_h \sum_i I_{h,i}$, where $\langle I_h \rangle$ is the mean intensity of a set of equivalent reflections. ‡ Mean figure of merit. § $R_{work} = \sum |F_{obs} - F_{calc}| / \sum F_{obs}$, where F_{obs} and F_{calc} are the observed and calculated structure-factor amplitudes. ¶ The R_{free} value was calculated with a random 10% subset of all reflections excluded from refinement.

In contrast to the periplasmic EcA-II, EcA-I was found to be a cytosolic enzyme that displays lower affinity for the substrate and was ineffective in inhibiting tumour growth (Schwarz *et al.*, 1966). Although these two isozymes catalyze an identical reaction, they can be distinguished by their solubilities in ammonium sulfate solution and by their sensitivity to thermal activation. *Saccharomyces cerevisiae* is also known to produce two L-asparaginase isozymes (ScA-I and ScA-II). ScA-I is a cytosolic enzyme, while ScA-II is an extracellular enzyme secreted in response to nitrogen starvation (Dunlop *et al.*, 1978). The two enzymes seem to interact in some way to regulate the utilization of asparagine as a nitrogen source for cell growth (Jones, 1977). Interestingly, the substrate-saturation response of ScA-I is sigmoidal, suggesting that ScA-I must be an allosteric enzyme (Dunlop *et al.*, 1978). Until now, no structures of type I L-asparaginase from any organism have been reported.

Recent genome projects have revealed that the hyperthermophilic archaeon *Pyrococcus horikoshii* contains only one L-asparaginase homologue protein (PhA). A BLAST search (Altschul *et al.*, 1997) has demonstrated that PhA is more similar to the eubacterial type I L-asparaginases than to the type II enzymes. The sequence of the PhA is 37% identical to EcA-I (positives, 52%; gap frequency, 4%), whereas it is 26% identical to EcA-II (positives, 45%; gap frequency, 6%). In this paper, we describe for the first time the crystal structure of PhA, a type I L-asparaginase-related enzyme. The structure of PhA provides us with some notable findings that have not been reported in previous structural studies of type II L-asparaginases.

2. Materials and methods

2.1. Overexpression and purification

The gene encoding PhA (*PH0066*) was amplified by polymerase chain reaction (PCR), purified using the QIAQuick PCR purification kit (Qiagen) and inserted into pET-26b(+) expression vector (Novagen) with *Nde*I and *Xho*I restriction-enzyme sites. *Escherichia coli* BL21-CodonPlus(DE3)-RIL (Stratagene) cells were transformed with the pET-22b(+)/PhA plasmid. The cells were grown at 310 K in 6 l LB medium containing 25 µg ml^{-1} kanamycin and 34 µg ml^{-1} chloramphenicol. Isopropyl-1-thio-β-D-galactopyranoside (IPTG) was added to a concentration of 0.5 m*M* to induce expression of PhA and the mixture was shaken for 12 h at 298 K. The cells were harvested by centrifugation at 4000*g* for 15 min at 277 K and resuspended in buffer *A* (50 m*M* Tris–HCl pH 9.0). The cells were disrupted by passage through a French pressure cell press at 8.3 MPa and the homogenate was clarified by centrifugation at 40 000*g* for 30 min at 277 K. The supernatant of the cell extract was incubated at 343 K for 30 min and centrifuged at 40 000*g* for 30 min. The supernatant was applied onto a HiTrap Q XL 5 ml anion-exchange column (Amersham Biosciences) that had been equilibrated with buffer *A*. After washing with buffer *A*, the bound proteins were eluted with a linear gradient of 0.0–1.0 *M* NaCl in 200 ml buffer *A*. The fractions containing PhA were pooled and then loaded onto a HiLoad 26/60 Superdex 200pg size-exclusion column (Amersham Biosciences) equilibrated with buffer *B* (50 m*M* Tris–HCl pH 9.0 and 300 m*M* NaCl). Finally, the sample was loaded onto a Resource PHE hydrophobic interaction column (Amersham Biosciences) equilibrated with buffer *A* containing 1 *M* ammonium sulfate (AS) and eluted with a decreasing linear gradient of AS. The protein eluted as a single peak. The fractions containing PhA were pooled and dialyzed against a solution containing 50 m*M* Tris–HCl pH 9.0 and 200 m*M* NaCl and concentrated using Amicon Ultra centrifugal filter devices (Millipore) to a final concentration of 10 mg ml^{-1}. For the production of selenomethionine (SeMet) substituted PhA, cells were cultured in minimal medium containing SeMet. The purification procedure for SeMet-substituted PhA was essentially the same as that for native enzyme.

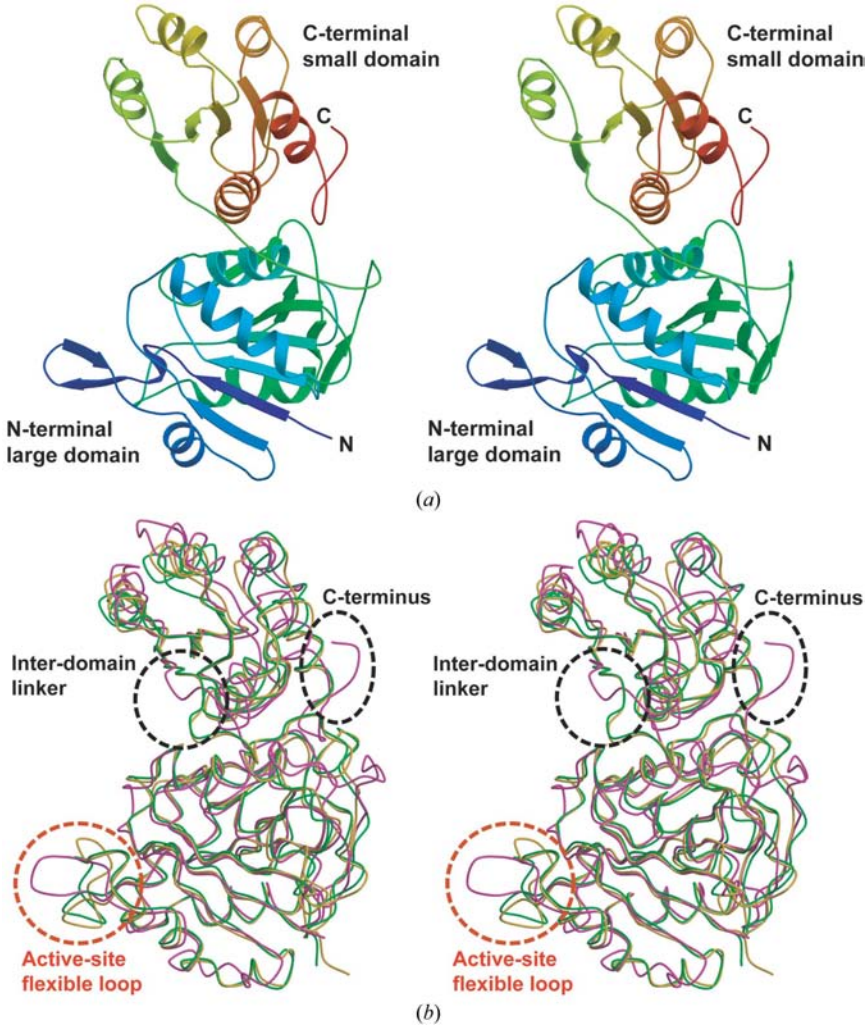

Figure 1
The structure of PhA. (*a*) Stereoview ribbon diagram of the PhA monomer. The structure of the PhA monomer can be divided into two domains: an N-terminal large domain and a C-terminal small domain. The model is coloured according to the sequence by a rainbow colour ramp from blue at the N-terminus to red at the C-terminus. (*b*) Stereoview of C^{α}-trace superimposition of PhA (pink), EcA-II (green; PDB code 3eca) and ErA (yellow; PDB code 1o7j). Three regions where structural differences were observed are marked with circles. The representations were generated using the programs *MOLSCRIPT* (Kraulis, 1991) and *RASTER3D* (Merritt & Bacon, 1997).

2.2. Crystallization and data collection

The initial crystallization trial was performed using the screening kits Crystal Screen, Grid Screen (Hampton Research) and Wizard Screen (Emerald Biostructures) and thin crystals of PhA were obtained under several conditions. After numerous attempts at optimization, the best single crystals were grown using the hanging-drop vapour-diffusion technique by mixing 2.0 µl protein solution and 1.0 µl reservoir solution containing 0.1 *M* Tris–HCl buffer pH 8.5, 12%(*v*/*v*) polyethylene glycol (PEG) 400 and 30 m*M* NaCl.

Prior to the X-ray diffraction experiment, the PhA crystals were rapidly soaked in the same solution supplemented with 25%(*v*/*v*) PEG 400 and flash-cooled under a nitrogen-gas stream at 100 K. The MAD data set was collected on beamline BL38B1 at SPring-8 (Harima, Japan) using a Quantum 4R charge-coupled device (CCD) detector (ADSC). Three wavelengths were selected based on the fluorescence spectrum of the Se *K* absorption edge, corresponding to the

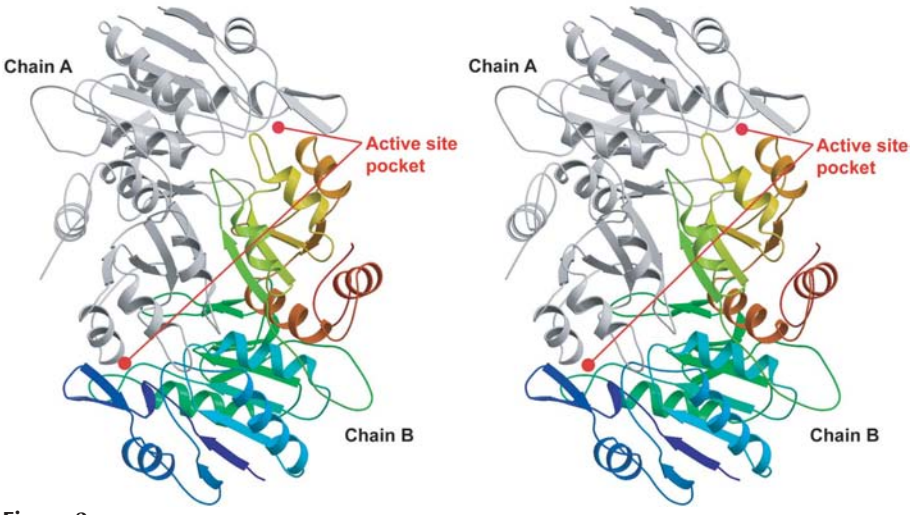

Figure 2
Stereoview ribbon diagram of the dimeric structure of PhA. One of the chains is coloured grey and the other by a rainbow colour ramp as in Fig. 1(*a*). The two active-site positions in the dimeric structure are roughly shown. The figure was generated using the programs *MOLSCRIPT* (Kraulis, 1991) and *RASTER3D* (Merritt & Bacon, 1997).

maximum f'' (peak, 0.9791 Å), the minimum f' (edge, 0.9794 Å) and the reference point (remote, 0.9000 Å). The diffraction data were indexed, integrated and scaled using the *HKL*2000 program package (Otwinowski & Minor, 1997). The PhA crystal used for the MAD data set (form I) was found to belong to the orthorhombic system $P2_12_12$, with unit-cell parameters a = 126.0, b = 76.5, c = 102.2 Å. In addition to the MAD data set, a higher resolution data set was also collected to a resolution of 2.16 Å on beamline BL41XU at SPring-8 using an R-AXIS V imaging plate (Rigaku). The data were also processed using the *HKL*2000 program package (Otwinowski & Minor, 1997). The crystal used for the higher resolution data set (form II)

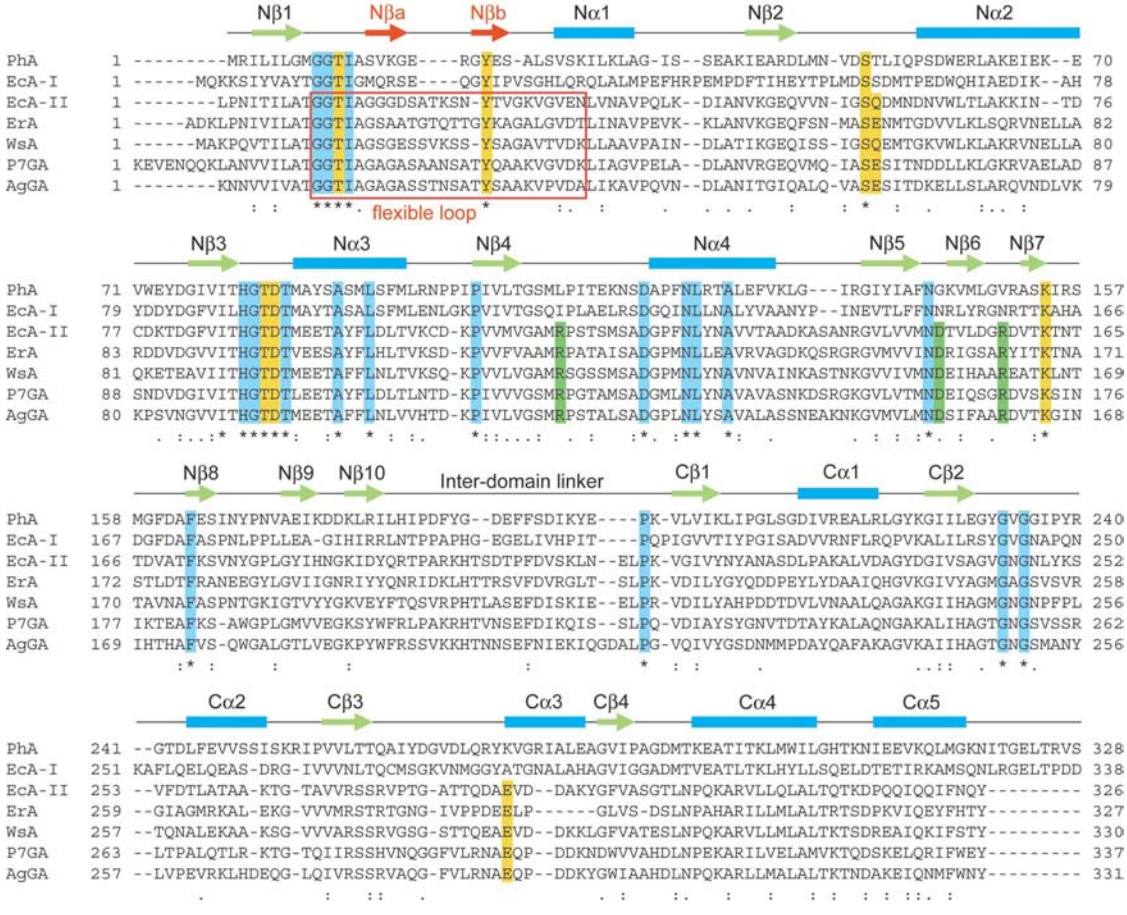

Figure 3
Structure-based sequence alignment among type I and II L-asparaginases. The completely conserved residues are coloured blue and the active-site residues are coloured yellow. The conserved residues of the type II enzymes that contribute to the interactions between two intimate dimers are also shown in green. PhA, *Pyrococcus horikoshii* L-asparaginase (type I); EcA-I, *Escherichia coli* L-asparaginase (type I); EcA-II, *E. coli* L-asparaginase (type II); ErA, *Erwinia chrysanthemi* L-asparaginase (type II); WsA, *Wolinella succinogenes* L-asparaginase (type II); P7GA, *Pseudomonas* 7A glutaminase-asparaginase (type II); AgGA, *Acinetobacter glutaminasificans* glutaminase-asparaginase (type II). Of these enzymes, only the structure of EcA-I has not yet been determined. The secondary-structure assignment of PhA is also given. The number of α-helices and β-strands is in accordance with that in the earliest paper describing the EcA-II (Swain *et al.*, 1993) and the two extra β-strands that appeared only in the PhA structure are designated Nβa and Nβb and coloured red. The alignment was partly performed using the program *CLUSTALW* (Thompson *et al.*, 1994).

belongs to the same space group $P2_12_12$, with slightly different unit-cell parameters: a = 125.7, b = 77.2, c = 98.7 Å.

2.3. Phasing and model refinement

The program *SOLVE* (Terwilliger & Berendzen, 1999) was used to determine the selenium sites and initial phase calculations were carried out using the program *SHARP* (de La Fortelle & Bricogne, 1997) using 17 of the 24 selenium sites. The residual selenium sites were determined by calculating the difference Fourier maps and five further selenium sites were determined. MAD phasing using the total of 22 selenium sites was performed with the program *SHARP* and the initial phases were improved by solvent flattening using the program *SOLOMON* (Abrahams & Leslie, 1996). The resultant electron-density map was not of sufficient quality to build the atomic model. Further phase improvement by multi-crystal averaging between form I and II as well as non-crystallographic symmetry (NCS) averaging was carried out using the program *DMMULTI* (Cowtan & Main, 1998). The improved experimental electron-density map was of high quality and 65.3% of the overall model was automatically built using the program *RESOLVE* (Terwilliger, 2000). To obtain a complete atomic model, further model building was semi-automatically performed using the program *LAFIRE* (local correlation-coefficient-based automatic fitting for refinement; manuscript in preparation) in combination with the refinement program *CNS* (Brünger *et al.*, 1998). At this point, the model was visually checked using the graphics program *O* (Jones *et al.*, 1991). Positional and individual *B*-factor refinement was accomplished using the program *CNS* (Brünger *et al.*, 1998), using higher resolution data ranging from 39.48 to 2.16 Å resolution. A randomly chosen 10% of all observed reflections were set aside for cross-validation analysis. A large NCS restraint weight (1256 kJ Å^{-2}) was applied in the early stages of model refinement and the weight was gradually decreased as refinement proceeded. The NCS restraint was finally released. After iterative cycles of model refinement and model corrections with *CNS* (Brünger *et al.*, 1998) and *LAFIRE*, the model was fitted manually using *O* (Jones *et al.*, 1991). The crystallographic *R* factor and free *R* factor ultimately converged. The programs *PROCHECK* (Laskowski *et al.*, 1993) and *WHATIF* (Vriend, 1990) were used to assess the quality of the final refined model.

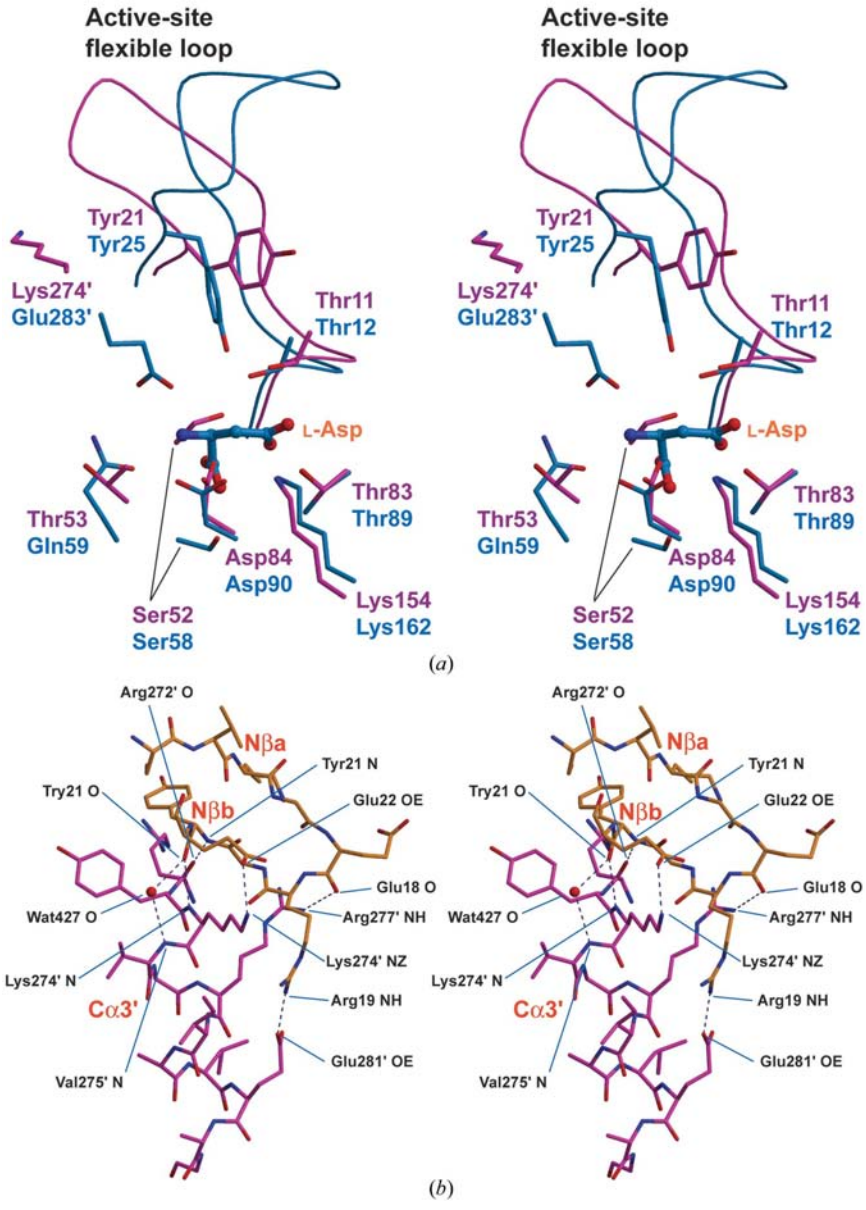

Figure 4
Active-site comparison between PhA and EcA-II. (*a*) Stereoview superimposition of the active-site residues of PhA (pink) and EcA-II (blue; PDB code 3eca). The active-site flexible loop is also shown. (*b*) Stereoview representation of the interactions between the stabilized loop (β-hairpin) and the α-helix derived from the other subunit of PhA. The β-hairpin and the α-helix are coloured yellow and pink, respectively. The figures were generated using the programs *MOLSCRIPT* (Kraulis, 1991) and *RASTER3D* (Merritt & Bacon, 1997).

3. Results and discussion

3.1. Overall structure

The structure of PhA was determined by the multiwavelength anomalous diffraction (MAD) method using the SeMet-substituted crystal and was refined to a resolution of 2.16 Å. The asymmetric unit was found to contain two PhA monomers (chains *A* and *B*) with a Matthews coefficient V_M of 3.30 Å^3 Da^{-1} (Matthews, 1968) and a solvent content of 62.5%. The final refined

model was composed of two complete polypeptide chains each consisting of 328 residues and 250 O atoms from solvent molecules. The model refinement was completed with a crystallographic R factor (R_{work}) and free R factor (R_{free}) of 21.1 and 25.3%, respectively. The data-collection and refinement statistics are summarized in Table 1.

The two chains in the asymmetric unit share a similar structure, with root-mean-square deviations (r.m.s.d.) for C^{α} and all atoms of 0.885 and 1.247 Å, respectively. The PhA monomer consists of two distinct α/β domains of different sizes connected by an extended linker which corresponds to residues 183–200 (Fig. 1*a*). The N-terminal large domain is folded as a flavodoxin-like motif and contains four α-helices (Nα1–Nα4) and 12 β-strands (Nβ1–Nβ10 and Nβa–Nβb). The core framework of the N-terminal domain is an eight-stranded β-sheet involving all four α-helices. There is a left-handed crossover between Nβ4 and Nβ5, which is rarely seen in protein structures (Richardson, 1981). The C-terminal small domain consists of five α-helices and a four-stranded parallel β-sheet (Cβ1–Cβ4). Two C-terminal α-helices (Cα4–Cα5) are located at the inter-domain side and the other three α-helices (Cα1–Cα3) are on the opposite side distal to the inter-domain interface.

The overall folding topology of the PhA is closely related to the previously reported structures of type II L-asparaginase (Fig. 1*b*). A pairwise structural comparison utilizing the DALI server (Holm & Sander, 1993) demonstrated that the r.m.s.d. of corresponding C^{α} atoms between PhA and EcA-II (PDB code 3eca) and between PhA and ErA (PDB code 1o7j) were 2.2 Å for 301 C^{α} atoms (Z score 34.6) and 2.1 Å for 290 C^{α} atoms (Z score 32.9), respectively. The low r.m.s.d. values indicate significant structural similarities, whereas the sequence identities over the fit regions were only 21 and 22%, respectively. Three regions were found where the main chain is not well superimposed on that of EcA-II and ErA. The first region is the linker connecting the two domains. The linker of PhA is highly extended and connects two domains *via* an even shorter route than that of EcA-II or ErA. The linker strain clearly arose from the deletion of seven residues compared with the sequence of type II L-asparaginase. The second part is seen around the C-terminal region. PhA has nine extra residues at the C-terminal end and the extra residues protrude from the globular body of the PhA monomer (Fig. 1*b*). The third structural difference is observed in a β-hairpin (Nβa–Nβb) that partially forms the active site. This is a novel finding because the β-hairpin corresponds to the so-called 'active-site flexible loop' of the type II L-asparaginases that plays a pivotal role in the initiation of catalysis (see §3.3).

3.2. Dimer assembly

Thus far, the crystal structures of type II asparaginase have without exception been reported as a homotetramer described as a 'dimer of intimate dimers' (Swain *et al.*, 1993) having 222 point-group symmetry. In contrast, the current structure clearly shows that the PhA only forms an intimate dimer and does not associate as a homotetramer (Fig. 2). However, this is not surprising as the active site in any tetrameric structure can be created with the residues belonging to the intimate dimer (Sanches *et al.*, 2003) and the association of two intimate dimers is not essential to the enzymatic function. It is considered that the PhA dimer is a minimum active unit that retains all the necessary conditions for activity.

The interface between the intimate dimers of EcA-II and ErA is created by hydrophobic interactions plus several hydrogen bonds and salt bridges (Sanches *et al.*, 2003). In contrast, a clear hydrophobic surface is not found in the corresponding region of PhA. Furthermore, several polar residues located at the interface between intimate dimers, such as Arg116, Asp152 and Asp158 of EcA-II, which are conserved in all type II L-asparaginases, are missing from the sequences of PhA and EcA-I (Fig. 3). These findings also indicate that the bacterial type I L-asparaginase must be present not as a homotetramer but as an intimate dimer. The dimeric structure of type I L-asparaginase is consistent with a previous inference based on sequence comparison (Bonthron & Jaskólski, 1997).

3.3. Active-site comparison

The substrate recognition and the catalytic mechanism of the type II L-asparaginase have been extensively investigated through a number of structural analyses of various enzyme–

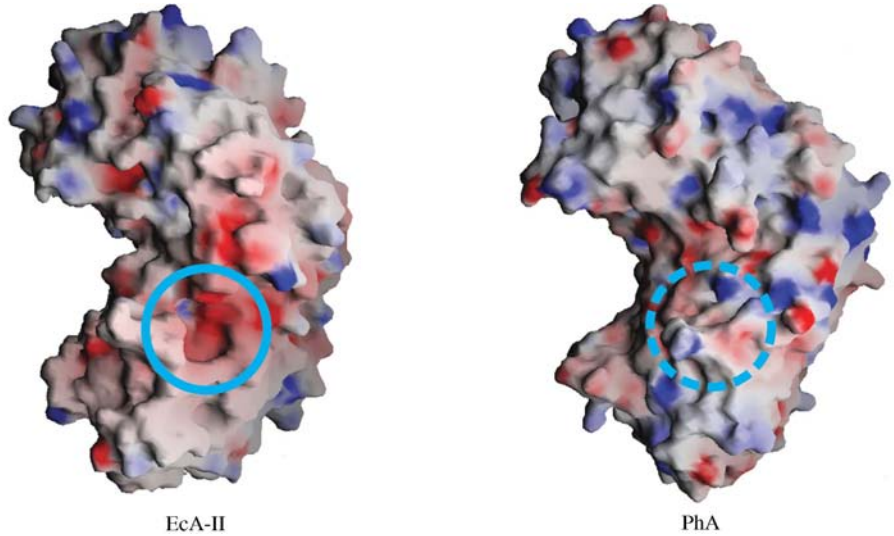

Figure 5
Molecular-surface representation of the unliganded EcA-II (PDB code 1ihd) and PhA. The molecular surface of both enzymes was calculated using the intimate dimer model. The active site of EcA-II is uncovered and exposed to the solvent (blue circle) owing to the flexibility of the loop region, while the active site of PhA is mostly covered with the inflexible β-hairpin structure (blue dotted circle). The molecular surfaces were generated with the program *GRASP* (Nicholls *et al.*, 1991).

ligand complexes and the highly conserved residues are found at the active site. In the case of EcA-II, these residues correspond to Thr12, Tyr25, Ser58, Gln59, Thr89, Asp90, Lys162 and Glu283′ (Figs. 3 and 4). Thr15 is known to be the first attacking nucleophile based on covalently bonded reaction-intermediate structures (Palm *et al.*, 1996; Ortlund *et al.*, 2000; Aghaiypour *et al.*, 2001*a*,*b*). The current structure shows that the residues corresponding to Gln59 and Glu283′ are substituted by threonine and lysine, respectively (Figs. 3 and 4*a*) and also that these two residues are not conserved in EcA-I (Fig. 3). In collaboration with Asp90, both Gln59 and Glu283′ serve as key residues that interact with the amino group of the substrate. The recognition mode for the substrate amino group somehow differs between the type I and type II enzymes.

The novel finding at the active site is that the conformation of the 'active-site flexible loop' is stabilized even though the active site is unoccupied by any ligands. The loop region has a high mobility and is partly or completely disordered in the structures of type II L-asparaginase (Lubkowski *et al.*, 1996). It is thus considered to play an important role as a 'mobile gate' for the active site (Jaskólski *et al.*, 2001). It should also be noticed that the loop contains residues Thr12 and Tyr25, which play crucial roles in the initiation of catalytic reaction. Therefore, loop flexibility is considered to be deeply involved in the enzymatic activity of the type II L-asparaginases. On the other hand, the structure of PhA unambiguously shows that the corresponding region is stabilized by β-hairpin formation and by elaborate interatomic interactions between Nβb and Cα3′ (Fig. 4*b*). In the structures of the type II enzyme, the α-helix corresponding to the Cα3 is very short or is missing owing to the deletion of two to six residues distancing these two segments. Therefore, the interaction between Nβb and Cα3′ seems to be specific for the type I enzyme. Although the loop stabilization gives rise to the loop's conformational change, it does not affect the position of the catalytically pivotal residues Thr11 and Tyr21. These two residues can be superimposed well on the corresponding residues Thr12 and Tyr25 of the EcA-II structure complexed with product L-aspartate, as shown in Fig. 4(*a*). The loop stabilization instead entails the complete loss of the loop's role as a mobile gate. Fig. 5 represents the molecular surfaces of unliganded EcA-II (PDB code 1ihd) and PhA. In the unliganded EcA-II structure most of the flexible loop is disordered (the model for residues 16–34 is not established) and the active-site pocket is seemingly exposed to the solvent. In contrast, the current structure clearly shows that the inflexible β-hairpin motif of the PhA shuts the active-site pocket and therefore access of substrate to the active site is expected to be limited. These observations may explain the lower affinity for the substrate of the type I L-asparaginases.

The authors would like to thank R. Ogawa of the Graduate School of Science at Hokkaido University for her kind help in protein purification. We also thank M. Kawamoto, H. Sakai and K. Hasegawa of the Japan Synchrotron Radiation Research Institute (JASRI) for their kind assistance with X-ray diffraction data collection on beamlines BL41XU and BL38B1 at SPring-8. This work was supported by a research grant from the National Project on Protein Structural and Functional Analyses from the Ministry of Education, Culture, Sports, Science and Technology of Japan.

References

Abrahams, J. P. & Leslie, A. G. W. (1996). *Acta Cryst.* D**52**, 30–42.
Aghaiypour, K., Wlodawer, A. & Lubkowski, J. (2001*a*). *Biochemistry*, **40**, 5655–5664.
Aghaiypour, K., Wlodawer, A. & Lubkowski, J. (2001*b*). *Biochim. Biophys. Acta*, **1550**, 117–128.
Altschul, S. F., Madden, T. L., Schaffer, A. A., Zhang, J., Zhang, Z., Miller, W. & Lipman, D. J. (1997). *Nucleic Acids Res.* **25**, 3389–3402.
Bonthron, D. & Jaskólski, M. (1997). *Acta Biochim. Pol.* **44**, 491–504.
Brünger, A. T., Adams, P. D., Clore, G. M., DeLano, W. L., Gros, P., Grosse-Kunstleve, R. W., Jiang, J.-S., Kuszewski, J., Nilges, N., Pannu, N. S., Read, R. J., Rice, L. M., Simonson, T. & Warren, G. L. (1998). *Acta Cryst.* D**54**, 905–921.
Cedar, H. & Schwartz, J. H. (1967). *J. Biol. Chem.* **242**, 3753–3755.
Cowtan, K. & Main, P. (1998). *Acta Cryst.* D**54**, 487–493.
Dunlop, P. C., Meyer, G. M., Ban, D. & Roon, R. J. (1978). *J. Biol. Chem.* **253**, 1297–1304.
Geuenich, S., Haberl, C., Egger, D., Kaspers, U., Hultner, L., Wilmanns, W. & Denzlinger, C. (1998). *Biochem. Pharmacol.* **55**, 447–453.
Holm, L. & Sander, C. (1993). *J. Mol. Biol.* **233**, 123–138.
Jakob, C. G., Lewinski, K., LaCount, M. W., Roberts, J. & Lebioda, L. (1997). *Biochemistry*, **36**, 923–931.
Jaskólski, M., Kozak, M., Lubkowski, J., Palm, G. & Wlodawer, A. (2001). *Acta Cryst.* D**57**, 369–377.
Jones, G. E. (1977). *J. Bacteriol.* **130**, 128–130.
Jones, T. A., Zou, J. Y., Cowan, S. W. & Kjeldgaard, M. (1991). *Acta Cryst.* A**47**, 110–119.
Kraulis, P. J. (1991). *J. Appl. Cryst.* **24**, 946–950.
La Fortelle, E. de & Bricogne, G. (1997). *Methods Enzymol.* **276**, 472–494.
Laskowski, R. A., MacArthur, M. W., Moss, D. S. & Thornton, J. M. (1993). *J. Appl. Cryst.* **26**, 283–291.
Lubkowski, J., Dauter, M., Aghaiypour, K., Wlodawer, A. & Dauter, Z. (2003). *Acta Cryst.* D**59**, 84–92.
Lubkowski, J., Palm, G. J., Gilliland, G. L., Derst, C., Rohm, K. H. & Wlodawer, A. (1996). *Eur. J. Biochem.* **241**, 201–207.
Lubkowski, J., Wlodawer, A., Ammon, H. L., Copeland, T. D. & Swain, A. L. (1994). *Biochemistry*, **33**, 10257–10265.
Lubkowski, J., Wlodawer, A., Housset, D., Weber, I. T., Ammon, H. L., Murphy, K. C. & Swain, A. L. (1994). *Acta Cryst.* D**50**, 826–832.
Mashburn, L. T. & Wriston, J. C. (1964). *Arch. Biochem. Biophys.* **105**, 450–452.
Matthews, B. W. (1968). *J. Mol. Biol.* **33**, 491–497.
Merritt, E. A. & Bacon, D. J. (1997). *Methods Enzymol.* **277**, 505–524.
Miller, M., Rao, M., Wlodawer, A. & Gribskov, M. (1993). *FEBS Lett.* **328**, 275–279.
Nicholls, A., Sharp, K. A. & Honig, B. (1991). *Proteins Struct. Funct. Genet.* **11**, 281–296.
Ortlund, E., Lacount, M. W., Lewinski, K. & Lebioda, L. (2000). *Biochemistry*, **39**, 1199–1204.
Otwinowski, Z. & Minor,W. (1997). *Methods Enzymol.* **276**, 307–326.
Palm, G. J., Lubkowski, J., Derst, C., Schleper, S., Röhm, K.-H. & Wlodawer, A. (1996). *FEBS Lett.* **390**, 211–216.
Richardson, J. S. (1981). *Adv. Protein Chem.* **34**, 167–339.
Röhm, K. H. & Van Etten, R. L. (1986). *Arch. Biochem. Biophys.* **244**, 128–136.

Sanches, M., Barbosa, J. A., de Oliveira, R. T., Abrahão Neto, J. & Polikarpov, I. (2003). *Acta Cryst.* D**59**, 416–422.
Schwartz, J. H., Reeves, J. Y. & Broome, J. D. (1966). *Proc. Natl Acad. Sci. USA*, **56**, 1516–1519.
Swain, A. L., Jaskolski, M., Housset, D., Rao, J. K. & Wlodawer, A. (1993). *Proc. Natl Acad. Sci. USA*, **90**, 1474–1478.
Terwilliger, T. C. (2000). *Acta Cryst.* D**56**, 965–972.
Terwilliger, T. C. & Berendzen, J. (1999). *Acta Cryst.* D**55**, 849–861.
Thompson, J. D., Higgins, D. G. & Gibson, T. J. (1994). *Nucleic Acids Res.* **22**, 4673–4680.
Vriend, G. (1990). *J. Mol. Graph.* **8**, 52–56.